Metastable Ions of the Noble Gases

HOMER D. HAGSTRUM
Bell Telephone Laboratories, Murray Hill, New Jersey
(Received June 5, 1956)

It is shown that ions of the noble gases in metastable excited states may be detected by their greater ability, with respect to the normal ion, to eject electrons from an atomically clean metal surface. The metastable ions are produced by a single electron impact with the parent normal atom. The ratio of cross sections for formation of the metastable and normal ions for argon, krypton, and xenon has been determined as a function of bombarding electron energy. At its maximum this ratio is about 0.02. The metastable ion must be observed over the "background" of normal ions in this method of detection, which is its inherent limitation. The relative number of helium ions formed in the $2\,^2S_{1/2}$ metastable state is below the detection sensitivity. It has been necessary to consider the nature of the interaction of a metastable ion with a metal surface, and an argument is given which indicates that the electron yield for the metastable singly-charged ion should be approximately equal to that measured for the doubly-charged ion.

I. INTRODUCTION

THE formation by electron impact of metastable ions[1] of the noble gases and the interaction of such ions with atomically clean metal surfaces are discussed in this paper. During the course of studies[2,3] of Auger-type neutralization and de-excitation of ions at metal surfaces, it was discovered that the ion beam in some instances contained a measurable fraction of ions in metastable excited states. These ions are produced by electron impact and are detected by their greater ability, with respect to unexcited ions, to eject electrons from the metal (Sec. III). The work reported here evaluates electron ejection from clean metals as a means of detection of metastable ions in other experiments in which they play a part (Sec. VIII).

Metastable ions have been observed in this work in argon, krypton, and xenon. Metastable states of sufficient lifetime do not exist in Ne^+. The failure to observe ions in the $2\,^2S_{1/2}$ state of He^+ is connected with the magnitudes both of the cross section for formation of the excited ion and the electron yield when this ion is neutralized and de-excited at a metal surface, relative to these quantities for the unexcited ion (Sec. VIII).

It has been shown (Sec. V) that the metastable ions are formed in a primary process involving a single electron impact with a noble gas atom. The dependence of cross section on electron energy can be derived from the data and the magnitude of the cross section determined if the cross section for formation of the unexcited ions and the electron yield for metastable ions at the metal surface are known (Secs. IV and VII). Consideration of the processes by which a metastable singly-charged ion and a normal doubly-charged ion each releases electrons from a metal leads one to the conclusion that the electron yields for these particles are very nearly equal (Sec. VI).

It is evident that one cannot produce a beam of ions consisting of one type merely by m/e analysis of the beam, or, in lieu of that, by operation of the electron beam in the ion source at an energy just below the second ionization energy.[4] In either case it is necessary to keep the bombarding electron energy below the threshold for the formation of the metastable ions. Since this was not done in the work published for tungsten,[2] some correction is necessary. In the accompanying paper,[5] data are published for Auger ejection of electrons from tungsten which are free from the effects of metastable ions.

II. NATURE OF EXPERIMENT AND APPARATUS

The experimental study of the ejection of electrons from metals by ions has been carried out in apparatus which may be schematically represented as shown in Fig. 1.[4] Here the ions are formed by electron impact in the parent gas in a magnetically collimated electron beam which passes through the apparatus at right angles to the initial direction of the ion beam (see "source end" in Fig. 1). In each instrument the ion beam is finally focussed on a ribbon target situated in the center of a

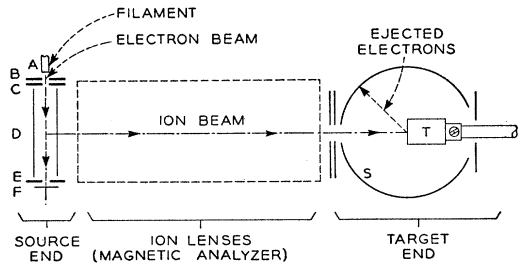

FIG. 1. Schematic representation of the apparatus used. See text in Sec. II.

[1] In this paper the term metastable ion is used to designate an ion which is in a metastable excited state. The term has also been applied to complex ions which fall apart into one or more atomic or molecular fragments during their flight through the apparatus. See Hipple, Fox, and Condon, Phys. Rev. **69**, 347 (1946); J. A. Hipple, Phys. Rev. **71**, 594 (1947); J. Phys. & Colloid Chem. **52**, 456 (1948).

[2] H. D. Hagstrum, Phys. Rev. **96**, 325 (1954).

[3] H. D. Hagstrum, Phys. Rev. **96**, 336 (1954).

[4] See discussion of instruments I or II, and III in H. D. Hagstrum, Rev. Sci. Instr. **24**, 1122 (1953).

[5] H. D. Hagstrum, Phys. Rev. **103**, 317 (1956), following paper.

spherical electron collector (see "target end" in Fig. 1). Between the source and target ends of the apparatus are lenses for focus and energy control of the ion beam. In one type of apparatus a mass analyzer is included and in another it is not. In the present work data have been taken with both types of instrument. The apparatus having a mass analyzer is instrument II of reference 4; that not having a mass analyzer is a newer instrument like instrument III of reference 4. This newer apparatus (instrument V) will not be discussed in detail here as it is planned to discuss it in a subsequent publication.

There are two basic measurements made in the study of Auger ejection processes. One is the measurement of electron yield (γ_{i1}) in electrons per incident singly-charged ion as it depends upon the type of ion, its kinetic energy at the target surface, and the state of cleanliness of the target surface. The second measurement is that of the energy distribution of ejected electrons, $N_0(E_k)$, as a function of the same parameters. The first measurement is made with the ejected electrons accelerated slightly from target to collector (V_{ST} being 2 volts negative), the second by retarding potentials between collector and target (V_{ST} positive). In the author's previous work, these measurements were made with the electron energy in the ion source just below the second ionization energy of the gas when an instrument without m/e analysis was used, and at any convenient energy when the ion beam was mass-analyzed. In the present work, the dependence of γ_{i1} and $N_0(E_k)$ on bombarding electron energy in the ion source is also studied.

The bombarding electron beam in the source is obtained thermionically from a filament (A in Fig. 1) and is accelerated through slits in electrodes B and C into the ionization chamber inside the electrode D. Electrodes C, D, and E are at the same potential. The total acceleration of the beam is thus given by the voltage, V_{AC}, between electrodes A and C, electrode B being placed at that intermediate potential which results in greatest beam intensity.

The experiment was conducted under the same conditions of vacuum, gas purity, and target cleanliness as the most recent of the author's previous work.[2] With liquid nitrogen on the traps, the background pressure was of the order of 3×10^{-10} mm Hg; with solid CO_2 and acetone on the traps (when A, Kr, and Xe were studied) the pressure was near 8×10^{-9} mm Hg. Monolayer adsorption time, using the target as adsorber, was monitored throughout the experiment. Measurements of yield were always made within 60 seconds after the target heating current was shut off after a flash. It has been demonstrated by the observation of the variation of γ_{i1} *versus* time after flash that the target was clean to within a few percent of a monolayer when measurements reported here were made.[2,4]

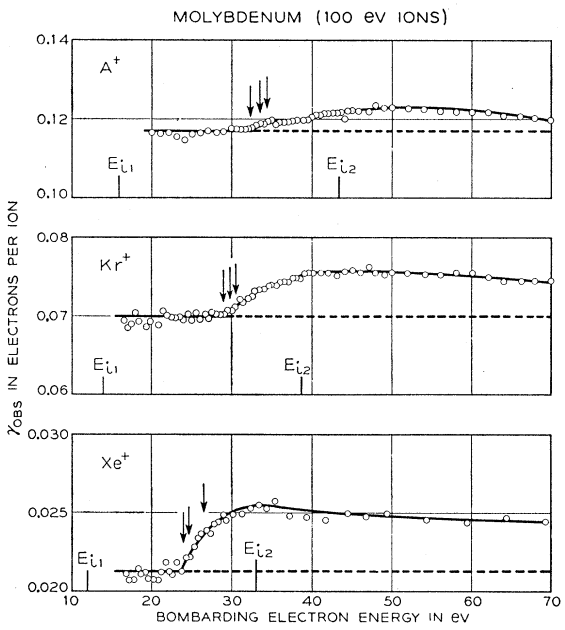

FIG. 2. Observed electron yields for A^+, Kr^+, and Xe^+ ion beams of 100-ev energy incident on atomically clean molybdenum plotted as functions of bombarding electron energy in the ion source. First and second ionization energies (E_{i1} and E_{i2}, respectively) are indicated. The arrows above each curve indicate the thresholds for formation of metastable ions (see Table I). The instrument used provided m/e analysis of the ion beam.

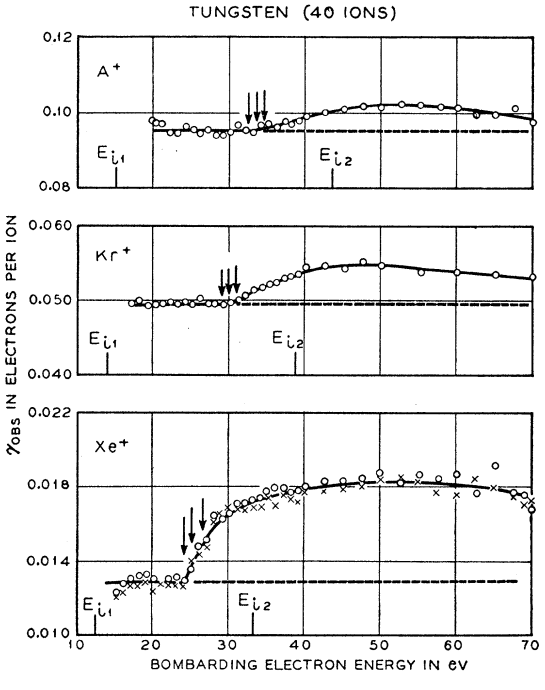

FIG. 3. Observed electron yields for A^+, Kr^+, and Xe^+ ion beams of 40-ev energy incident on atomically clean tungsten plotted as functions of bombarding electron energy in the ion source. The arrows above each curve indicate the thresholds for formation of metastable ions (see Table I). As the instrument used for these measurements did *not* provide m/e analysis, there is a small admixture of doubly-charged ions in the beam at energies greater than E_{i2}. The two sets of data shown for Xe^+ were taken at pressures in the ion source differing by a factor of 28.

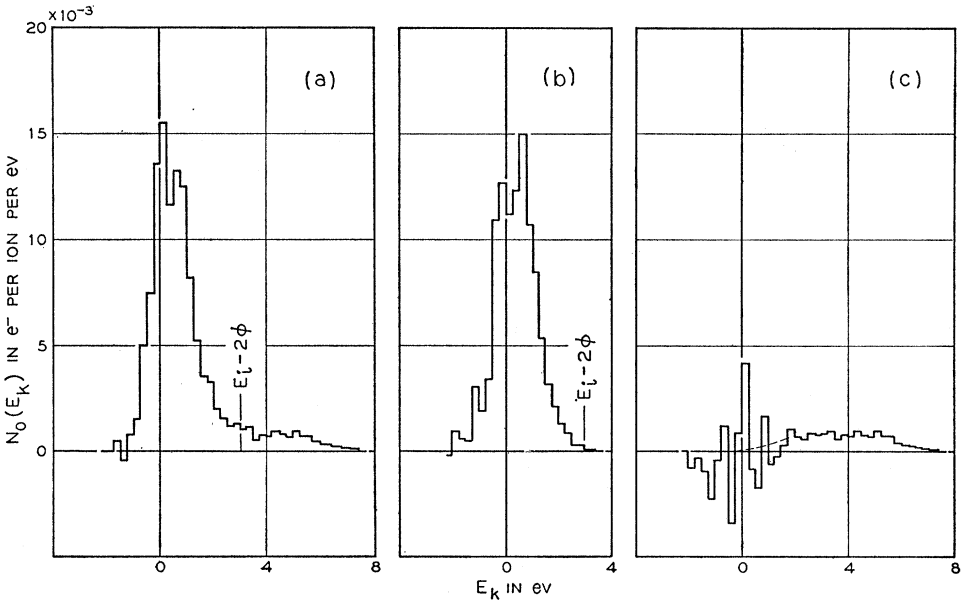

FIG. 4. Energy distribution functions of electrons ejected from molybdenum by a beam of singly-charged xenon ions. (a) $N_0(E_k)$ for a bombarding electron energy (V_{AC}) of 35 ev near the maximum of the γ_{obs} curve for Xe^+ of Fig. 2. This distribution includes electrons ejected by the metastable ion Xe^{+m} as well as the normal ion Xe^+. (b) $N_0(E_k)$ for bombarding electron energy of 22 ev, that is, just below the threshold for formation of metastable ions. (c) Difference between curves in graphs (a) and (b).

As the bombarding electron energy is reduced toward the first ionization energy, E_{i1}, the intensity of the ion beam is reduced by virtue of the diminishing ionization cross section and eventually becomes too low for accurate measurement. For this reason, the data given here are all for values of $V_{AC}>E_{i1}+5$ volts.

III. DETECTION OF THE METASTABLE IONS

Before describing the method of detecting the metastable ions, it is instructive to consider what one would expect if they were *not* present. Since both electron yield, γ_{i1}, and the energy distribution, $N_0(E_k)$, are quantities defined per incident ion, one would expect each to be independent of the means of formation of the ion beam and its intensity. In particular, γ_{i1} and N_0 would be expected to be independent of V_{AC} at energies sufficiently above E_{i1} to produce a beam of manageable intensity. With m/e analysis this should extend to any energy, without such analysis to the second ionization energy, E_{i2}.

The presence of the metastable ions in the ion beam is most strikingly seen in a plot of observed electron yield γ_{obs} as a function of the energy of the bombarding electrons in the ion source. Figures 2 and 3 are plots of such data for each of the singly-charged ions of argon, krypton, and xenon incident on clean molybdenum and tungsten, respectively. Here γ_{obs} is seen *not* to be independent of electron energy in the source as one would expect if only normal ions were present. γ_{obs} is constant only up to those energies above which metastable ions can be formed, above which γ_{obs} increases with bombarding electron energy, passes through a broad maximum, and then decreases. As we shall see, this can only result from a change in the composition of the beam above the threshold (Sec. IV). Below the threshold, γ_{obs} must equal γ_{i1}.

If one looks at the energy distribution of ejected electrons as a function of bombarding electron energy, one sees a picture consistent with the variation of γ_{obs}. In Fig. 4, typical $N_0(E_k)$ functions for Xe^+ on molybdenum are plotted for two values of bombarding electron energy, V_{AC}. In Fig. 4(a) is shown $N_0(E_k)$ for $V_{AC}=35$ volts, that is, near the maximum deviation of γ_{obs} from γ_{i1}. The $N_0(E_k)$ function has a tail at the high-energy end which extends considerably beyond the approximate upper limit $E_{i1}-2\varphi$ (φ is the work function of the metal) for electrons ejected in the process of Auger neutralization.[6] This tail is never greater than 4 to 5% of the maximum of the $N_0(E_k)$ distribution. Earlier measurements were not taken at sufficiently small increments of V_{ST} nor were they extended far enough beyond $E_i-2\varphi$ to establish the effect conclusively. In Fig. 4(b) is shown $N_0(E_k)$ for $V_{AC}=22$ volts, that is, just below the threshold for formation of the metastable ions. Here we see that the tail has disappeared and that the distribution function is "well behaved" in the sense that it is what one should expect for simple Auger neutralization of the normal ion.[6] This behavior of $N_0(E_k)$ is further evidence that γ_{obs} for V_{AC} less than the metastable threshold is equal to γ_{i1} and that above the threshold another beam constituent capable of ejecting more and faster electrons from the target has appeared. In Fig. 2(c) the difference between the distributions of Fig. 2(a) and Fig. 2(b) are plotted. The significance of this distribution is discussed further in Sec. VI.

[6] The reader is referred to reference 3 for a discussion of the Auger processes for unexcited, singly-charged ions incident on clean metal surfaces.

TABLE I. Energy levels in the noble gases.[a]

	He	Ne	A	Kr	Xe
Ground state of atom	$^1S_0$; 0	$^1S_0$; 0	$^1S_0$; 0	$^1S_0$; 0	$^1S_0$; 0
Ground state of singly-charged ion	$^2S_{1/2}$; 24.58	$^2P_{3/2}°$; 21.56	$^2P_{3/2}°$; 15.76	$^2P_{3/2}°$; 14.00	$^2P_{1/2}°$; 12.13
Metastable states of ion	$^2S_{1/2}$; 65.38	...	$^4D_{7/2}$; 32.16 $^4F_{9/2}$; 33.38 $^4F_{7/2}$; 33.45 $^2F_{7/2}$; 34.25	$^4D_{7/2}$; 28.90 $^4F_{9/2}$; 29.62 $^4F_{7/2}$; 29.86 $^2F_{7/2}$; 30.32	$^4D_{7/2}$; 23.96 $^4F_{7/2}$; 24.38 $^4F_{9/2}$; 24.45 $^2F_{7/2}$; 26.37
Ground state of doubly-charged ion	78.98	$^3P_2$; 62.63	$^3P_2$; 43.38	$^3P_2$; 38.56	$^3P_2$; 33.34

[a] Energies are given in electron volts. Data taken from C. E. Moore, *Atomic Energy Levels*, National Bureau of Standards, Circular No. 467 (U. S. Government Printing Office, Washington, D. C., 1949), Vol. I (He, Ne, A); Vol. II (1952) (Kr); H. H. Landolt and R. Börnstein, *Tables* (Springer-Verlag, Berlin, 1950), Vol. 1, Part 1 (Xe).

A^+, Kr^+, and Xe^+ each possess four metastable states, $^4D_{7/2}$, $^4F_{9/2}$, $^4F_{7/2}$, $^2F_{7/2}$ (see Table I). These states are metastable with respect to the ground state of the ion ($^2P_{3/2}°$ for A^+ and Kr^+, $^2P_{1/2}°$ for Xe^+) by virtue of the selection rule on ΔJ, and with respect to all lower lying excited states by virtue of Laporte's rule. Quadrupole and magnetic dipole radiations have transition probabilities in the range 1 to 10^{-4} sec^{-1} compared to 10^6 to 10^8 sec^{-1} for dipole radiation.[7] Unless multiple quantum transitions are important, the metastable states in A^+, Kr^+, and Xe^+ should thus have lifetimes greater than 1 sec. The longest transit time through the experimental apparatus used here is about 30 μsec.

In Ne^+ there are no metastable states like those in the heavier noble gas ions. The $^4P-^2P°$ intercombination lines near 21 900 cm^{-1} are of intensity $\frac{1}{2}$ to $\frac{1}{4}$ that of the most intense line of the Ne II spectrum reported by Boyce.[8] We note in Fig. 5 that no deviation of γ_{obs} from a constant value (γ_{i1}) is observed for Ne^+. Neither is any such deviation observed for He^+ even though a metastable state ($2\,^2S_{1/2}$) does exist in He^+. As has been said, failure to observe this state results (1) because the metastable ion in helium is formed with somewhat lower probability than are metastable ions in the heavier noble gases, and (2) because the electron yield for the metastable ion He^{+m} relative to that for the normal ion He^+ is smaller than is this ratio for the heavier ions. Further discussion of these points and numerical estimates are given in Sec. VIII. The estimates of Novick, Lipworth, and Yergin[9] indicate that the lifetime of $He^{+m}(2\,^2S_{1/2})$ is sufficiently long for the present experiment and cannot account for the failure to observe the metastable ion here.[10] In the cases of A^{+m}, Kr^{+m}, and Xe^{+m} it is possible that the decay mechanisms involving two quanta discussed by Breit and Teller[11] for He^{+m} will reduce the metastable lifetime below the values estimated for quadrupole and magnetic dipole radiation. This is unimportant here as it is an experimental fact that the metastable ions are sufficiently long-lived to be observed in the present experiment.

IV. RELATION OF THE OBSERVED YIELD (γ_{obs}) TO ION BEAM COMPOSITION

We discuss now the relation of the observed yield (γ_{obs}) to the composition of the beam and to the cross section for formation of the metastable ions. We have already indicated that, since the beam is composed entirely of singly-charged ions, the increase in γ_{obs} seen in Figs. 2 and 3 can result only from an increase in the relative proportion in the beam of a type of singly-charged ion which has greater ability than the normal ion to release electrons from the target. The only such particle is an ion in a metastable excited state. Let us denote the fraction of the beam which is thus excited as f_{im}. We shall not distinguish the several metastable levels in this discussion. If γ_{i1} and γ_{im} are the total electron yields for normal and excited ions, respectively, we expect γ_{obs} to be given by the relation

$$\gamma_{obs}=(1-f_{im})\gamma_{i1}+f_{im}\gamma_{im}. \quad (1)$$

From (1), assuming no loss of metastability by Stark quenching in the ion beam, we obtain the fraction f_{im}, which is related to the ratio of the cross sections, thus

$$f_{im}=Q_{im}/(Q_{i1}+Q_{im})=(\gamma_{obs}-\gamma_{i1})/(\gamma_{im}-\gamma_{i1}). \quad (2)$$

Here Q_{i1} is the cross section for formation of the normal ion, Q_{im} that for the metastable ion. If, as we expect,

[7] See E. U. Condon and G. Shortley, *The Theory of Atomic Spectra* (Cambridge University Press, Cambridge, 1935). Quadrupole and magnetic dipole radiations are discussed on page 283 and lifetimes with respect to dipole radiation are listed in Table 5[5] on page 136.

[8] J. C. Boyce, Phys. Rev. 46, 378 (1934).

[9] Novick, Lipworth, and Yergin, Phys. Rev. 100, 1153 (1955). Of the times listed in their Table II, only the natural decay and Stark quenching times are of interest here. No stronger Stark quenching is expected in the present work than in these Lamb-shift experiments.

[10] R. Novick (private communication) has given the lifetime of the $2\,^2S_{1/2}$ state, considering coupling to the $P_{1/2}$ state and neglecting that to the $P_{3/2}$ state, to be $1.4\times10^{-2}/E^2$ sec (E in volts/cm). Use of E near 10 volts/cm gives a lifetime of 100 μsec to be compared with the maximum transit time through the apparatus of 30 μsec. Collision quenching is negligible at the pressures obtaining in this experiment.

[11] G. Breit and E. Teller, Astrophys. J. 91, 215 (1940).

$Q_{im} \ll Q_{i1}$,

$$f_{im} \cong Q_{im}/Q_{i1} \cong (\gamma_{obs}-\gamma_{i1})/(\gamma_{im}-\gamma_{i1}). \quad (3)$$

Since $(\gamma_{im}-\gamma_{i1})$ is a constant for any given combination of ion and metal target, we expect Q_{im} to be proportional to the deviation of γ_{obs} from γ_{i1} if Q_{i1} may be taken as constant over a range of bombarding electron energies. $(\gamma_{obs}-\gamma_{i1})$ in Figs. 2 and 3 does have the form expected for a cross section as a function of bombarding electron energy. We shall see that the data taken for a molybdenum target and a tungsten target give the same value of f_{im}.

V. PRIMARY NATURE OF THE FORMATION PROCESS

It has been possible to demonstrate that the metastable ions are formed as primary products of a single electron impact with the parent noble gas ion. In Fig. 3 two sets of data for γ_{obs} *vs* bombarding electron energy are given for Xe^+. These were taken at pressures in the ionization chamber differing by a factor of 28 as judged from pressure measurements in the target chamber of the apparatus. Although absolute pressures in the ion source cannot be specified accurately, they are approximately 2.8×10^{-4} and 1.0×10^{-5} mm Hg for the two curves. The fact that $(\gamma_{obs}-\gamma_{i1})$ is the same in the two cases indicates that the process giving rise to the metastable ion is unimolecular.

γ_{obs} for Xe^+ on molybdenum was also measured as a function of density in the bombarding electron beam. The best measure of electron beam density is the ion beam intensity at constant pressure since variation of filament temperature does not maintain a constant density across the beam. In Fig. 6, γ_{obs} is plotted against ion beam current. Electron beam energy (V_{AC}) was 35 ev corresponding to the maximum deviation of γ_{obs} from γ_{i1} (Fig. 2). The fact that γ_{obs}, and thus Q_{im}, is independent of electron density in the bombarding beam over nearly two orders of magnitude can only mean that the formation of the Xe^{+m} involves only a single electron impact.

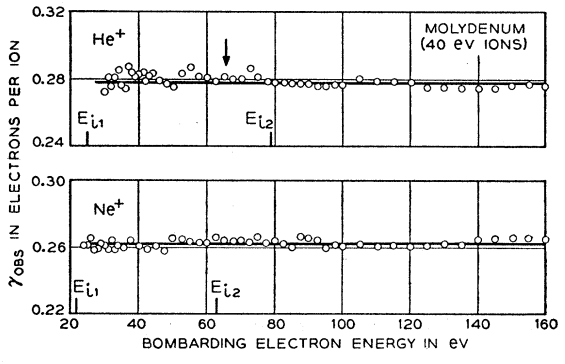

FIG. 5. Plots of observed electron yield for He^+ and Ne^+ ion beams of 40-ev energy incident upon atomically clean molybdenum as functions of bombarding electron energy in the ion source. First and second ionization energies are indicated. The arrow above the He^+ curve indicates the threshold energy for formation of $He^{+m}(2\,^2S_{\frac{1}{2}})$ at 65.39 ev. The instrument used provided m/e analysis of the ion beam.

VI. ELECTRON YIELD (γ_{im}) FOR THE METASTABLE ION

Equation (2) of Sec. IV relates the fraction f_{im} of metastable ions present in the beam to the three yield parameters, γ_{obs}, γ_{i1}, and γ_{im}. γ_{obs} is the measured total yield for the beam which consists of a mixture of normal and metastable ions. γ_{i1} is the yield parameter for normal ions only and is obtained as the constant value of γ_{obs} below the threshold for formation of metastable ions. γ_{im}, the yield of electrons ejected per metastable ion striking the target, is unobtainable in this experiment. However, a value for it is needed if f_{im} or Q_{im} is to be determined. It is the purpose of this section to estimate γ_{im} by showing that it should be very nearly equal to the measured yield for doubly-charged ions, γ_{i2}.

The argument for the approximate equality of γ_{im} and γ_{i2} rests upon the proposition that a doubly-charged ion, on approaching a metal surface sufficiently slowly, will be partially neutralized to an excited state of the singly-charged ion before any Auger-type process can occur. If such a resonance transition occurs first then subsequent Auger-type processes in which electrons are released will be very similar to those which would occur if the particle incident on the surface were initially a metastable singly-charged ion.

An energy level diagram which depicts the situation for xenon and tungsten is shown in Fig. 7. Potential energy of a test electron is plotted vertically, the energy of a free electron at rest an infinite distance from the metal being taken as zero. The metal is shown at the left, the stippled region indicating the allowed energy band lying between the energies $-\varphi$ and $-\epsilon_0$. The atomic particle lies at a distance s from the metal surface. The energy levels for the xenon particle are those of an electron moving about the doubly-charged Xe^{++} ion core. These are thus the ground and excited levels of Xe^+. The two lowest lying excited levels are shown as dashed lines, the ground state and the four metastable levels as full lines. In the stippled region

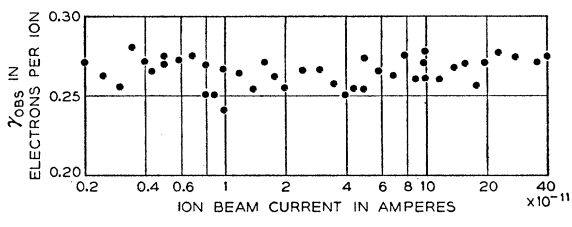

FIG. 6. Variation of γ_{obs} as a function of electron beam intensity. The plot is made against ion beam current as the best measure of bombarding electron beam intensity. The curve was taken at an electron beam energy of 35 ev (V_{AC}) at which $(\gamma_{obs}-\gamma_{i1})$ is maximum (Fig. 2).

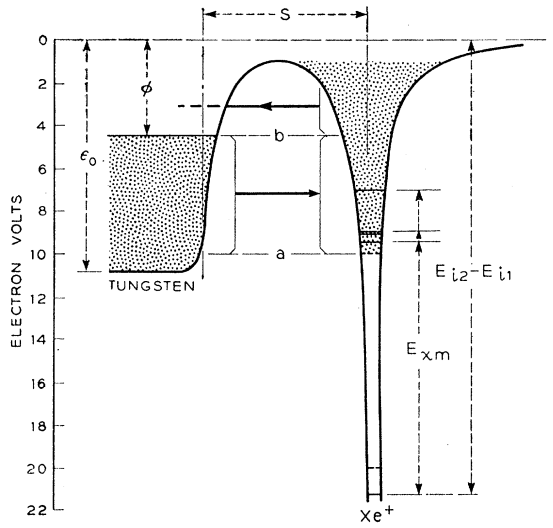

FIG. 7. Energy level diagram indicating resonance transitions of electrons which can occur between the metal tungsten and the singly-charged ion Xe^+. Resonance transitions which neutralize Xe^{++} to Xe^{+*} can occur at energy levels between *a* and *b*. Resonance transitions which ionize Xe^{+*} can occur only at levels above *b*. Metastable levels are indicated by full lines, lowest excited levels by dashed lines, and the region of excited levels in Xe^+ by stippling. The conduction band in tungsten is also indicated by stippling. Energy level shifts when the ion is near the metal surface have been neglected in drawing this diagram.

there is a rather high density of excited, nonmetastable levels.

If the particle approaching the metal surface is Xe^{++}, none of the levels of Xe^+ in Fig. 7 are filled. The proposition stated above then says that the first electronic process to occur as Xe^{++} approaches the surface is a resonance tunneling from the filled band in the metal into an excited level in the atomic ion. Such transitions can occur for energies lying between the levels *a* and *b* indicated in the figure. The excited electron in the singly-charged ion thus formed may fill one of the metastable levels but is more likely to occupy one of the higher excited levels to which the tunneling process is more probable. However, the energy level of the excited ion, Xe^{++}, can differ from that of a metastable ion, Xe^{+m}, by no more than about 4 volts out of a total excitation energy of about 12 volts above the ground state of the singly-charged ion for xenon (Table I).

Auger-type processes take place closer to the metal surface than the resonance tunneling and involve de-excitation and neutralization which take the particle Xe^{+*} to the ground state of the parent atom, Xe. Since these processes for the excited ion, Xe^{+*}, formed from Xe^{++} by resonance tunneling should be the same as those occurring if the particle were initially a metastable ion, Xe^{+m}, we conclude that $\gamma_{im} \cong \gamma_{i2}$. Even though the specific nature of these processes is immaterial to the present argument, it can be stated that in all probability they consist of Auger de-excitation of Xe^{+*} to Xe^+ followed by Auger neutralization of Xe^+ to Xe. Further discussion of these matters will be included in a paper on Auger ejection from molybdenum to be published soon.

We conclude that the probability of a resonance transition is greater at a given distance from the metal than that of an Auger-type process for the doubly-charged ion because this appears strongly to be the case for singly-charged ions. As discussed in Sec. XI of reference 3, both theory and experiment bear out the conclusion that resonance transitions from the metal into excited states of the neutral atom or from such states into the metal to produce the singly-charged ion are more probable than are the Auger-type processes when the atomic particle is at a given distance from the metal surface.

Confirmation of the picture presented above is obtained by comparing the energy distributions, $N_0(E_k)$, of electrons ejected by Xe^{+m} and by Xe^{++}. The first of these is obtained as the difference between N_0 functions measured with and without metastable ions present in the beam. This difference function for Xe^{+m} on molybdenum is plotted in Fig. 4(c) and as the curve labeled ($Xe^{+m} \rightarrow Xe^+$) in Fig. 8. Since each particle in the beam is a singly-charged ion which is thought to be finally neutralized in the process of Auger neutralization taking Xe^+ to Xe, the difference function should give the energy distribution of only those electrons released in the de-excitation of the metastable ion to the ground state of the singly-charged ion. The corresponding function for Xe^{++}, representing the electrons released when Xe^{++} goes to Xe^+, is obtained as the measured N_0 function for Xe^{++} ions minus that for Xe^+ ions. This second difference function is plotted as the curve

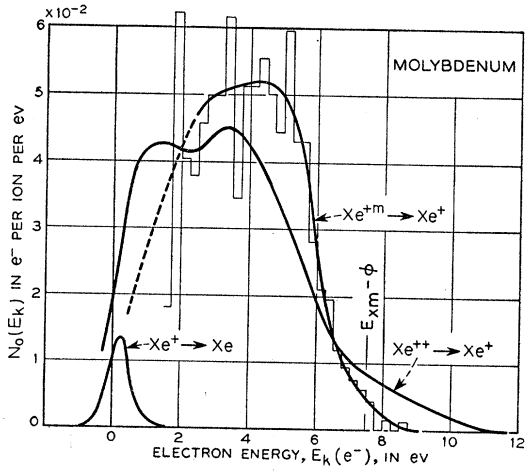

FIG. 8. Energy distribution functions for electrons ejected from molybdenum in the various stages involved in the neutralization and de-excitation of the metastable ion and the doubly-charged ion of xenon. The curve labeled $Xe^+ \rightarrow Xe$ is that measured for Xe^+ ions and corresponds to the final stage for each of the above processes. The curve labeled ($Xe^{+m} \rightarrow Xe^+$) is the curve of Fig. 2(c) normalized to the same area as the ($Xe^{++} \rightarrow Xe^+$) curve. The curve labeled ($Xe^{++} \rightarrow Xe^+$) is the N_0 distribution measured for Xe^{++} ions minus the ($Xe^+ \rightarrow Xe$) curve.

labeled ($Xe^{++}\rightarrow Xe^{+}$) in Fig. 8. For comparison the N_0 function for Xe^{+}, labeled ($Xe^{+}\rightarrow Xe$), is also shown. The ($Xe^{+m}\rightarrow Xe^{+}$) curve has been normalized to the same area as that under the ($Xe^{++}\rightarrow Xe^{+}$) curve.

We note that the curves for ($Xe^{++}\rightarrow Xe^{+}$) and ($Xe^{+m}\rightarrow Xe^{+}$) in Fig. 8 are quite similar, indicating that similar Auger processes are involved. This lends support to the view that in each case the electrons are ejected in an Auger process which de-excites an excited ion to the ground state of the ion.

The maximum kinetic energy of electrons ejected by Auger de-excitation of the lowest Xe^{+m} level should be very close to the value $E_{xm}-\varphi$. For Xe^{+} and molybdenum, $E_{xm}-\varphi=11.83-4.27=7.56$ ev. This value should be reduced only very little if the van der Waals' forces are taken into account and increased by about 2 ev by virtue of energy level shifts and the Heisenberg principle. We note that the upper limit of the Xe^{+m} curve in Fig. 8 does lie somewhat above the value of $E_{xm}-\varphi$. We also note that there are faster electrons in the distribution for Xe^{++} in Fig. 8 than in that for Xe^{+m}. This is perhaps evidence that a least some of the electrons from the metal which partially neutralize the arriving Xe^{++} ions, tunnel into excited levels which are higher than the metastable levels. $E_x-\varphi$ for the highest possible excited level is equal to $E_{i2}-E_{i1}-2\varphi$, which for Xe and molybdenum is $21.08-8.54=12.54$ ev.

Finally, the reasonableness of the contention that $\gamma_{im}\cong\gamma_{i2}$ is shown by a calculation based on the theory of Auger de-excitation previously published.[3] One can calculate a value for the electron yield $(\gamma_{im}-\gamma_{i1})$ resulting from Auger de-excitation of the xenon metastable ion to the normal ion. This yields $(\gamma_{im}-\gamma_{i1})=0.22$, which may be compared with the experimental values for $(\gamma_{i2}-\gamma_{i1})$ of 0.21 for tungsten and 0.23 for molybdenum (Table II). The theoretical value may be expected to be quite accurate because the electron energy distribution for the process $Xe^{+m}\rightarrow Xe^{+}$ lies in the same energy range as that for the process $He^{+}\rightarrow He$ to the data for which the theory was originally fitted.[3]

TABLE II. Comparison of various yield parameters for tungsten and molybdenum targets (40 ev ions).

		A	Kr	Xe
γ_{i1}[a]	W	0.095	0.049	0.013
	Mo	0.118	0.065	0.021
γ_{i2}[a]	W	0.40	0.30	0.22
	Mo	0.41	0.34	0.25
$\gamma_{obs}-\gamma_{i1}$[b]	W	0.005	0.004	0.004
	Mo	0.005	0.005	0.004

[a] These data are taken from published work on tungsten, references 2 and 5, and from work soon to be published for molybdenum.
[b] This quantity is a function of bombarding electron energy and is given here for $V_{AC}=E_{i2}$ from Figs. 2 and 3.

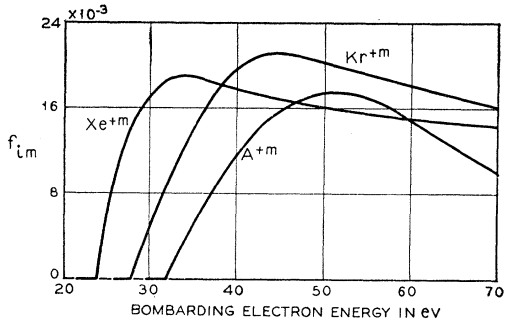

FIG. 9. Plots of fraction $f_{im}\cong Q_{im}/Q_{i1}$ as a function of bombarding electron energy determined from the measured curves of Figs. 2 and 3 as described in the text.

VII. CROSS SECTION FOR FORMATION OF METASTABLE IONS BY ELECTRON IMPACT

If we now take $\gamma_{im}=\gamma_{i2}$, we are in a position to calculate f_{im} by Eq. (2) of Sec. IV. In order to determine the absolute magnitude of Q_{im}, however, we must know both γ_{im} and Q_{i1}. Since Q_{i1} has been determined only for A^{+} of the gases A, Kr, and Xe, we shall leave the cross-sectional data here in the form of f_{im}. The γ_{i2} values used are listed in Table II. Curves of f_{im} *vs* bombarding electron energy, determined from the γ_{obs} curves of Figs. 2 and 3, are plotted in Fig. 9. Very little difference was found between the data taken for molybdenum and tungsten. Note the equality of $\lambda_{obs}-\lambda_{i1}$ values for tungsten and molybdenum listed in Table II. This is as it should be for, although f_{im} is expressible in terms of electron yields from a specific metal surface, the value of f_{im} must be independent of the surface used.

We note that f_{im} near its maximum is about 2% for each of the three gases. For A, this can be translated into a value for Q_{im} since Q_{i1} has been measured. Data on Q_{i1} are summarized by Massey and Burhop.[12] The cross-sectional data are obtained by combining the measurements of Bleakney[13] with those of Smith.[14] Bleakney's data on A^{+} show that Q_{i1} has a maximum at 50-ev electron energy. At 30 ev, Q_{i1} is down only to 70%, and at 70 ev to 95% of its maximum value. Thus Q_{i1} for argon is quite constant over the electron energy range for which f_{im} is plotted in Fig. 9. If we take Q_{i1} to be constant over the range of Fig. 9 at its maximum value of 3.2×10^{-16} cm^2, we find for argon

$$Q_{im}(\mathrm{A})=3.2\times10^{-16}f_{im}. \qquad (4)$$

It is of interest to note from Fig. 9 that the form of the cross section as a function of electron energy presents a broader maximum for a process of simultaneous excitation and ionization than is found for the

[12] H. S. W. Massey and E. H. S. Burhop, *Electronic and Ionic Impact Phenomena* (Clarendon Press, Oxford, 1952), Table I on p. 38.
[13] W. Bleakney, Phys. Rev. 36, 1303 (1930).
[14] P. T. Smith, Phys. Rev. 36, 1293 (1930).

TABLE III. Figure of merit for detection of metastable ions by Auger ejection in the presence of normal ions.

Ion	He^{+m}	A^{+m}	Kr^{+m}	Xe^{+m}
$(\gamma_{im}-\gamma_{i1})/\gamma_{i1}$ [a]	1.62	2.42	4.25	10.9

[a] It has been assumed that $\gamma_{im}=\gamma_{i2}$, and the measured γ_{i2} and γ_{i1} values from the molybdenum work to be published elsewhere have been used.

process of excitation alone.[15] The curves observed here are sharper, however, than the excitation and ionization function obtained for $He^{+m}(2\,^2S_{1/2})$ by Novick, Lipworth, and Yergin[9] (their Fig. 15).

Lamb and Skinner[16] have estimated by the so-called sudden approximation method the cross-section Q_{im} for the $2\,^2S_{1/2}$ state of He^+. They obtain the ratio of Q_{im} to Q_{i1} of 0.01 [their equation (32)]. It is interesting that this is close to the 0.02 figure obtained in this work for the same ratio in A, Kr, and Xe. It must be remembered, however, that $f_{im}=0.02$ includes population of the metastable levels by transitions from higher lying nonmetastable states. Thus it should be larger than a value representing only transitions directly from the ground state to the metastable levels. Lamb and Skinner have also estimated Q_{i2}/Q_{i1} by the same methods and obtain a ratio of 0.011 to be compared with Bleakney and Smith's[17] measured value of 0.005. Although this is excellent agreement, it may indicate that the theoretical estimate of Q_{im}/Q_{i1} is somewhat high. This has a bearing on the failure to detect He^{+m} in the present work. These matters are discussed further in the next section.

VIII. AUGER EJECTION AS A MEANS OF DETECTING METASTABLE IONS

We discuss finally the use of Auger ejection as a means of detecting metastable ions. The method depends upon the fact that the metastable ion ejects more electrons and of different kinetic energy than those ejected by the singly-charged ion. The method as used here has the serious disadvantage, however, that there is present the "background" of electrons ejected by the normal ion. The success of the method depends on the ability to detect the change in electron yield caused by the appearance of the metastable ion against this background. Thus it must depend on the magnitude of the parameter $(\gamma_{obs}-\gamma_{i1})/\gamma_{i1}$. From Eq. (2), taking $\gamma_{im}=\gamma_{i2}$, we obtain

$$(\gamma_{obs}-\gamma_{i1})/\gamma_{i1}=f_{im}(\gamma_{im}-\gamma_{i1})\gamma_{i1}. \quad (5)$$

As expected, this depends on the fraction of metastable ions in the beam and on a factor $(\gamma_{im}-\gamma_{i1})/\gamma_{i1}$ which depends solely on the characteristics of the means of detecting the presence of the metastable ions. The factor $(\gamma_{im}-\gamma_{i1})/\gamma_{i1}$ may thus be taken as a sort of figure of merit of the detecting means. Values of $(\gamma_{im}-\gamma_{i1})/\gamma_{i1}$ have been calculated for the metastable, singly-charged ions of the noble gases taking $\gamma_{im}=\gamma_{i2}$. These are tabulated in Table III. We note that the figure of merit increases toward the heavier noble gases. This is principally the result of the reduction of γ_{i1}, which, in turn, results from the lower values for E_{i1}. We may conclude in general that the method of detecting metastable ions by Auger ejection is more successful the smaller γ_{i1}, that is, the less important the ejection of electrons by the normal ion becomes. A metastable ion is detectable if $(\gamma_{obs}-\gamma_{i1})/\gamma_{i1}$ is greater than the minimum detectable change in observed yield. In the present work, this is of the order of 2%. In the case of argon (see Figs. 2 and 3), a 5% change in γ_{obs} is readily detectable.

We are now in a position to say why the $He^{+m}(2\,^2S_{1/2})$ ion was not observed in the present work. Using Lamb and Skinner's cross-section ratio Q_{im}/Q_{i1} discussed in the last section, we calculate from Eqs. (3) and (5), using the figure of merit given for He in Table III, that

$$\left[\frac{(\gamma_{obs}-\gamma_{i1})}{\gamma_{i1}}\right]_{He^{+m}(2\,^2S_{\frac{1}{2}})}=0.016. \quad (6)$$

This is just about at the limit of sensitivity of the method. In any event, the failure to observe $He^{+m}(2\,^2S_{1/2})$ in the present experiment may be used to set an upper limit on Q_{im}/Q_{i1} for this state in He^+ of about 0.01, the value estimated by Lamb and Skinner.

ACKNOWLEDGMENTS

The author wishes to acknowledge in particular the help of C. D'Amico who not only operated the apparatus and recorded all the data for the present work but who also first measured the crucial dependence of γ_{obs} on bombarding electron energy. Thanks are also due N. B. Hannay, R. Novick, D. J. Rose, and P. A. Wolff for helpful discussions and critical reading of the manuscript.

[15] See, for example, the work of R. Dorrestein, Physica **9**, 433, 447 (1942). This and other work on excitation functions are summarized in Chap. II of Massey and Burhop.[12]

[16] W. E. Lamb, Jr., and M. Skinner, Phys. Rev. **78**, 539 (1950). Appendix II.

[17] W. Bleakney and L. G. Smith, Phys. Rev. **49**, 402 (1936).